Journal of Cellular Physiology

Ex Vivo Assay of Electrical Stimulation to Rat Sciatic Nerves: Cell Behaviors and Growth Factor Expression

ZHIYONG DU,[1,2] OLEXANDR BONDARENKO,[2] DINGKUN WANG,[2] MAHMOUD ROUABHIA,[3] AND ZE ZHANG[2]*

[1]*Qiandongnan National Polytechnic, Kaili, China*

[2]*Département de chirurgie, Faculté de médecine, Centre de recherche du CHU de Québec, Université Laval, Québec (QC), Canada*

[3]*Groupe de recherche en écologie buccale, Faculté de médecine dentaire, Université Laval, Québec (QC), Canada*

Neurite outgrowth and axon regeneration are known to benefit from electrical stimulation. However, how neuritis and their surroundings react to electrical field is difficult to replicate by monolayer cell culture. In this work freshly harvested rat sciatic nerves were cultured and exposed to two types of electrical field, after which time the nerve tissues were immunohistologically stained and the expression of neurotrophic factors and cytokines were evaluated. ELISA assay was used to confirm the production of specific proteins. All cell populations survived the 48 h culture with little necrosis. Electrical stimulation was found to accelerate Wallerian degeneration and help Schwann cells to switch into migratory phenotype. Inductive electrical stimulation was shown to upregulate the secretion of multiple neurotrophic factors. Cellular distribution in nerve tissue was altered upon the application of an electrical field. This work thus presents an ex vivo model to study denervated axon in well controlled electrical field, bridging monolayer cell culture and animal experiment. It also demonstrated the critical role of electrical field distribution in regulating cellular activities.

J. Cell. Physiol. 231: 1301–1312, 2016.

Electrical stimulation (ES) has been shown to promote neurite outgrowth in vitro and nerve regeneration in animals (Jiang et al., 2013; Marquardt and Sakiyama-Elbert, 2013) as well as accelerate peripheral axon growth in clinic trials (Gordon et al., 2009). The efficacy of ES is thought to take place through the upregulation of multiple neurotrophins (English et al., 2007; Geremia et al., 2007). In peripheral nerve injury, neurotrophins in the nerve stump distal to the injury are mostly secreted by proliferating Schwann cells which participate in the Wallerian degeneration and serve to guide the regenerating axons (Fawcett and Keynes, 1990; Scherer and Salzer, 2001). However, the temporal and spatial effect of ES on cellular activities and neurotrophin production inside denervated nerve tissue has not been well understood.

While the response of Schwann cells to ES can be studied in a cell culture environment (Nguyen et al., 2013; Forciniti et al., 2014; Luo et al., 2014), in vivo they respond to injury and ES while interacting with other cell populations such as fibroblasts, endothelial cells and macrophages and residing in their natural tissue scaffold. Conventional cell culture therefore does not provide an ideal environment to study how denervated cell populations respond to ES. Koppes et al. (2011) co-cultured neurons with Schwann cells and reported the synergic effect of Schwann cells and ES to neurite growth, showing that electrically stimulated Schwann cells may help peripheral nerve growth.

Intrinsically conductive polymers are a class of synthetic materials with both electrical conductivity and ionic activity (Wallace et al., 2003). Polypyrrole (PPy), the most studied conductive polymer, has been shown to support a variety of cell types including neurons, and be compatible with different tissues including nerve (Balint et al., 2014). Nerve channels made of conductive polymers provide uniform electrical fields within a well-defined boundary. These polymeric channels can be as flexible and compliant as soft tissue, and be of biodegradable design. Compared to such insulating organic materials as biodegradable polycaprolactone or collagen, conductive polymeric channels can deliver ES, evidently. A recent example is the chitosan/PPy channel reportedly improved the functional recovery of rats following sciatic nerve injury when treated with ES (Huang et al., 2012).

We previously reported that nerve channels made of polylactide (PLLA)/PPy membrane supported neuron growth in vitro and sciatic nerve regeneration in rats (Zhang et al., 2007). We then developed conductive textiles and demonstrated their capacity to mediate pulsed ES to human skin fibroblasts (Wang et al., 2013). Compared to the PLLA/PPy membrane, conductive textile remains soft, flexible and suturable. This conductive textile was used to construct two

Zhiyong Du and Olexandr Bondarenko authors made equal contributions to this article.

Contract grant sponsor: The Canadian Institutes of Health Research Operating Grant;
Contract grant number: MOP 106555.
Contract grant sponsor: Centre de recherche du CHU de Québec.

*Correspondence to: Ze Zhang, Centre de recherche de l'Hôpital Saint-François d'Assise, 10 rue de l'Espinay, Québec (QC) G1V 3L5, Canada. E-mail: ze.zhang@chg.ulaval.ca

Manuscript Received: 11 August 2015
Manuscript Accepted: 28 October 2015

Accepted manuscript online in Wiley Online Library (wileyonlinelibrary.com): 30 October 2015.
DOI: 10.1002/jcp.25230

types of nerve channels to determine the cellular reactions of freshly harvested sciatic nerves to ES. Because of the preservation of cell populations and tissue structures, this ex vivo tissue culture model is expected to better resemble the situation in vivo than monolayer culture of Schwann cells, and the ES parameters identified in the experiment may be translated to pre-clinical studies.

Materials and Methods

Conductive textile preparation

The conductive textile was made of poly(ethylene terephthalate) (PET) fabric surface coated with PPy (Wang et al., 2013). Woven PET fabric (Testfabrics Inc., West Pittston, PA) was first cut into specimens $2 \times 4\ cm^2$ in size and cleaned. The PET specimens were then transferred into a methanol/water (50/50 vol/vol) solution containing pyrrole monomers (10% w/v) (Alfa Aesar, Ward Hill, MA), followed by incubation for 30–45 min. The specimens were then bathed in a ferric chloride ($FeCl_3$, Laboratoire Mat, Québec, QC, Canada) (10% w/v) solution of methanol in water (50:50) for about 15 min to complete the polymerization reaction.

Scanning electron microscopy (SEM)

The surface morphology of the PPy-coated fabric was observed under a Jeol JSM-6360LV scanning electron microscope (Soquelec Inc., Montréal, QC, Canada) at an accelerating voltage of 15 kV. The specimens were sputter coated with gold to facilitate observation.

Surface electrical resistivity of the PPy-coated fabric

The electrical resistivity of the fabric specimens was measured with a standard four-point method using a Jandel Multiheight Probe (Jandel Engineering, Linslade, Bedfordshire, UK). The diameter of the probes was 500 μm, with a separation of 1 mm. All of the specimens were measured under constant probe pressure and identical humidity which was approximately 60%. At least 5 specimens were measured at multiple locations.

Nerve channels

Two types of nerve channels were constructed based on different ES principles. The first type was called a conductive channel which consisted of a cylindrical tube 10 mm in length and 1.5 mm in diameter sutured from a rectangular conductive fabric. Two strips of fabric extended from both ends of the tube, passed through the edge of a cell culture Petri dish and connected with an electrical power source, as shown in Figure 1A. When introduced into the electrical circuit, electrical current entered from one end, passed through the tube and exited out the other end. No ionic current was present inside the tissues in this ES model. The second type was called an inductive channel, consisting of two pieces of parallel rectangular conductive fabrics, as illustrated in Figure 1B. The fabrics were 10 mm long and 3 mm wide and the space between them was 1.5 mm created by two silicone spacers. The two fabrics extended outside of the Petri dish to connect with the power source. Upon ES, an electrical field was established between the two parallel fabrics, which may induce ionic movement and the polarization of inducible chemical groups in the tissues sandwiched between the fabrics.

Sterilization

Figure 1 shows the nerve channels assembled into the Petri dishes. The assemblies were sterilized by ethylene oxide (EO) at 55°C according to standard procedures.

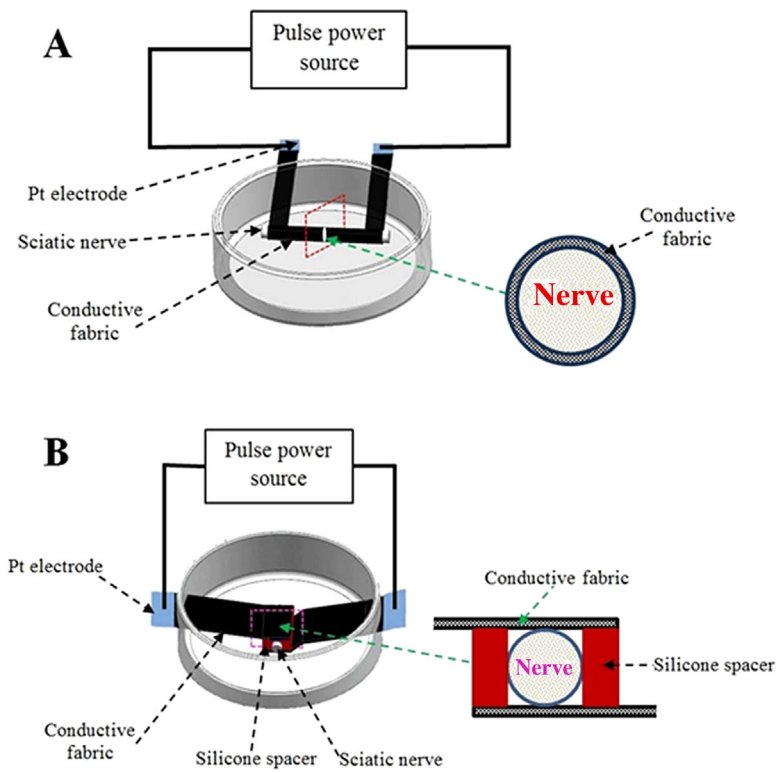

Fig. 1. Illustration of the two different never guidance channels: (A) conductive nerve channel; (B) inductive nerve channel.

Sciatic nerve harvesting

Twenty-two sciatic nerves 15 mm in length were harvested from eleven female Sprague–Dawley rats weighing 250–300 g immediately following their sacrifice. Once the loosely attached connective tissue was removed, the nerves were cut into 10 mm-long sections, individually weighed and subsequently used for the tissue culture experiments. The total time between animal sacrifice and the beginning of the culture experiments was less than 24 h. The nerves were kept in antibiotic-supplemented culture medium at 4°C until use.

Tissue culture

The nerve segments were either gently introduced into the tubular conduits (conductive channels) or sandwiched between the two separated fabrics (inductive channels). A predetermined volume of culture medium (Dulbecco's Modified Eagle Medium/Ham's F-12 nutrient mixture, 1:1) (DMEM/F-12) containing 1% penicillin/streptomycin and 10% fetal bovine serum (FBS) was added to completely cover the nerve channel. The nerves harvested from the right side were electrically stimulated while those from the left side were used as controls which were cultured under the same conditions but without ES. All of the cultures were carried out in a standard culture incubator at 37°C in 5% CO_2. At the end of the experiment, all of the nerve specimens were carefully removed from the channels, weighed again and cut into segments for histological and immunohistological analyses. A quantitative assessment of different growth factors was performed on tissue lysates.

ES

Four nerves were electrically stimulated for 24 h and one for 48 h using the conductive channels. For the inductive channels, three nerves were stimulated for 24 h and another three for 48 h. An equal number of nerves were used in control experiment, that is, cultured in the same type of conductive channels with no electricity applied. A Grass S88 dual output square pulse stimulator (Grass Instruments Co., Quincy, MA) was used to generate a pulse of 160 mV/mm (along the length of the conductive channels) or 200 mV/mm (across the separation of the two fabric capacitors of the inductive channels) in intensity, 200 μs in pulse width and 2 Hz in frequency for the entire duration of the tissue culture. To connect the stimulator and the conductive channel, two thin platinum films were attached to the two ends of the PPy-coated PET fabric outside of the Petri dish, with no contact with the culture medium. The out put channels of the stimulator are directly connected to the platinum films. The selection of these two ES intensities was based on our previous work and literatures. Because of the different nerve channel configurations, the two ES intensities are not comparable.

Histology

After accomplishing the ES, nerve stumps were detached from the conduits, harvested and fixed in 4% formaldehyde in PBS at pH 7.4 for 12 h under gentle agitation. The fixed specimens were then washed in distilled water and dehydrated in ethanol solutions of increasing concentrations up to 100%. For the paraffin-embedded specimens, the proximal and distal stumps were sectioned transversally and the middle longitudinally. At least three 3-μm-thick sections were cut from each specimen and colored either with toluidine blue, Masson-Goldner trichrome, or immunohistochemical stains. To detect cell attachment to the fabrics and potential mineral deposits, the specimens of the conduits were also harvested, fixed in 4% formaldehyde and embedded in PMMA-based resin embedding medium (Leica Historesin) for 24 h under agitation and vacuum at room temperature. The resin blocks were sectioned in 3 μm thickness and stained with toluidine blue and Prussian blue.

Immunohistochemistry

Ten mono- and polyclonal primary antibodies were used: mouse monoclonal anti-S-100 (clone 4C4.9, Acris Antibodies, San Diego, CA), rabbit monoclonal anti-Ki67 (clone SP6, Acris Antibodies), rabbit polyclonal anti-NGF (Acris Antibodies), mouse monoclonal anti-CD56 (clone 123C3, Acris Antibodies), rabbit polyclonal anti-BDNF (Acris Antibodies), rabbit polyclonal anti-FGF-1 (Novus Biologicals, Oakville, ON, Canada), rabbit polyclonal anti-FGF-2 (Novus Biologicals), rabbit polyclonal anti-GDNF (Novus Biologicals), rabbit polyclonal anti-CNTF (Abcam, Toronto, ON, Canada), and mouse monoclonal anti-p75 (clone MC192, Abnova, Taipei, Taiwan, China). Each slice was deparaffinized, rehydrated, and treated with 70% methanol and 0.5% H_2O_2 for 30 min at room temperature to block endogenous peroxidase. After washing in PBS (pH 7.4), the heat-induced antigen retrieval was performed in a microwave oven (700 W) for 30 min in citrate buffer (pH 6.0) with 0.05% Tween 20. Thereafter, the slices were treated with blocking serum (normal chicken serum, Vector Labs, Burlingame, Ca) for 20 min to prevent non-specific binding of secondary antibodies and subsequently incubated with the primary antibodies overnight at 4°C. Each slice was then incubated with the biotinylated chicken anti-mouse or anti-rabbit immunoglobulins (Novus Biologicals) and then with ABC-solution (Vectastain ABC-Kit, Vector Laboratories, Burlingame, CA) at room temperature for 40 min. The DAB substrate kit (Vector Laboratories) was used for visualization followed by a counterstaining with Gill's haematoxylin. Positive controls were performed using the sections of rat brain tissue and native sciatic nerves. Negative control sections, in which the primary antibody was replaced by PBS, were also included in all staining runs. Following the dehydration and mounting, a histological analysis of the slices was performed as described below.

Histological evaluation and morphometry

All of the sections were examined by a trained pathologist at least three times by means of a Zeiss AxioPlan microscope (Zeiss GmbH, Oberkochen, Germany) at magnifications of ×100, ×200, and ×400. A qualitative assessment of the immunohistochemical stains was performed based on the visual observations of the occurrences of the oxidized DAB deposition and their distribution in the sample. The immunostaining of the S100 protein was performed for the precise detection of Schwann cells, which were counted in six different fields of view (FOV) at a magnification of ×400. The fields of view were chosen for the maximal coverage of nerve's cross section. In that way the cell counting areas always embraced the segments from perineurium to the central direction of each sample. The FOVs immediately adjacent to perineurium were defined as peripheral region. Ki67 expression was a typical proliferative index calculating the percentage of positive nuclei among the total number of cells in the same population. The measurement of the staining intensity and the counting of nuclei and cells were performed using Image-Pro 6.0 software (Media Cybernetics, Rockville, MD).

ELISA assay of neurotrophic factor secretion

The concentrations of neurotrophic factors found to be upregulated in the immunohistochemistry analysis were further quantified through sandwich enzyme-linked immunosorbent assay (ELISA). Tissue extracts were prepared according to standard protocols. Briefly, a predetermined quantity of nerve tissue (5 mg) was homogenized by means of an ultrasonic processor (Sonics & Materials, Newtown, CT) in a known volume (ex. 300 μl) of complete extraction buffer with protease and phosphatase

inhibitor cocktails and then shaken for 2 h at 4°C, after which time the tubes were centrifuged for 20 min at 13000 rpm at 4°C and the supernatants were transferred into chilled tubes and stored at −80°C for analysis. The following neurotrophic factors were analyzed: CNTF and NGF ELISA kits from Abcam (ab100758 and ab100757, Abcam, Cambridge, MA), GDNF and BDNF ELISA kits from Novus Biologicals (BEK-2020-2P and BEK-2000-2P, Novus Biologicals), and FGF1 and FGF2 ELISA kits from QAYEE-BIO (QY-E11073 and QY-E10310, QAYEE-BIO, Shanghai, China). The plates were read at 450 nm and analyzed using a microplate reader (μQuant, Bio-Tek, Winooski, VT).

Statistics

A student *t*-test was used to calculate the significance of difference in the mean values between the experimental and the control groups. A Mann–Whitney U test was performed for the evaluation of cellular asymmetry significance within each investigated group. The level of significance was selected at $P < 0.05$.

Results

The conductive fabrics

Under SEM, the coating appeared thin and smooth without blocking the interstitial space (Wang et al., 2013). Macroscopically, the conductive fabrics appeared to be uniformly coated and retained the handling property and suturability of the original fabric. The average surface electrical resistivity of the conductive fabrics was found approximately 18 kΩ per square, which is normal for such a small amount of PPy coating. There was no any morphological change in fabric channels following experiment. As for the electrical conductivity, the current decreased from the initial 134 microA to 112 microA in the first 24 h and then flattened in conductive channels, showing a marginal decrease in conductivity. For the inductive channels, the current increased from the initial 0.1 to 2.5 microA during measurement, showing a significant increase in electroactivity.

Gross examination of the nerve tissue

Following inductive ES, the diameter of the nerve stumps appeared to be larger (data not shown). They also recorded a significant increase in weight compared to the control and the conductive ES groups (Table 1), with the weight of the nerves in the control groups decreasing slightly.

General histology

Similar microscopic patterns were found in both the ES and the control groups, including a fragmentation and formation of "bead-like" structures in degrading axons, and a vacuolization in the axoplasm in the entire length of the nerve fascicles. In addition, mast cells were identified at an aggregation of approximately five cells per transversal section. Macrophages were found in all of the samples as large (15 μm) cells with abundant cytoplasm and one round nucleus with a distinct nucleolus. The average number of macrophages in any sample was no more than 1–2 cells per section area and signified no meaningful difference among samples.

Masson-Goldner trichrome staining. A change in cell nuclei was observed in the control groups, with a swelling of nuclei in some neurolemmocytes and a condensing of chromatine along the nuclear membrane. Similar nuclear features were found in one conductively stimulated sample which showed Schwann cells with well-shaped nucleoli, although well-shaped nucleoli in both Schwann cells and fibroblasts were abundantly present in inductive ES samples at 48 h (Fig. 2). No sufficient signs of cellular pathology were found except for the occasional presence of necrotic cells in the matrix and interstitial edema (Fig. 2).

Toluidine blue staining. The intensity of the endoneurium staining with toluidine blue represented the amount of myelin remnants during Wallerian degeneration. It was noted that the increased time of tissue culture was associated with a decrease in endoneural staining intensity. Moreover, all of the electrically stimulated samples, particularly the inductive ES groups, exhibited weaker staining compared to the control groups, as shown in Figure 2. This indicated that ES, particularly inductive ES, accelerated Wallerian degeneration.

Immunohistochemistry

S100 protein expression and Schwann cell morphometry. S100 protein is a well-known marker of neuroectodermal differentiation. In this study, it was used as a specific marker of neurolemmocytes (Schwann cells) which are the only population of neuroectodermal origin in the peripheral nervous system. As shown in Figure 2, S100 protein displayed both intracellular and nuclear immunolocalizations. While all of the samples exhibited moderate to strong expression in Schwann cells, the occasional appearance of S100 within the axial cylinders was detected after 24 and, more notably, 48 h of inductive ES. In comparison, the occurrence and intensity of S100-positive zones in the samples of the control and conductive ES groups were insufficient inside of the neurites and moderate in Schwann cells.

Schwann cell number. A significantly increased number of neurolemmocytes (S100-positive) was observed following 24 h of ES, regardless of the type of nerve channel, as presented in Table 1; however, this difference disappeared at 48 h due to the increase in S100-positive cells in the control groups.

Schwann cell distribution. Four fields of view at ×400 both adjacent to the perineurium and in the central area of nerve tissue were examined using Image-Pro 6.0 software. Schwann cell distribution was calculated as the average ratio of "peripheral" to "central" neurolemmocytes (P/C) in the proximal, middle, and distal segments of the nerve stumps (Table 1). A clear feature was that the P/C ratio in the ES groups was larger than 1 as early as 24 h, meaning a preferential distribution of Schwann cells in the perineurium. A similar P/C ratio was observed in the control groups only at 48 h.

TABLE 1. Schwann cell morphometry and weight change in nerve stumps

	Control groups				ES groups							
					Inductive				Conductive			
Hours of culture	Cells/FOV	P/C	Δm ($g \times 10^{-4}$)	No. of nerves	Cells/FOV	P/C	Δm ($g \times 10^{-4}$)	Number of nerves	Cells/FOV	P/C	Δm ($g \times 10^{-4}$)	Number of nerves
24	20 ± 7	1.1	−25 ± 7	7	41 ± 11	1.7	37 ± 19	3	39 ± 17	1.8	n/a	4
48	40 ± 11	1.5	−11 ± 8	4	42 ± 16	1.7	64 ± 26	3	40 ± 14	1.5	n/a	1

FOV, field of view; P/C, ratio of Schwann cells peripheral to that at the nerve center; Δm, mass difference before and after culture; n/a, data not available.

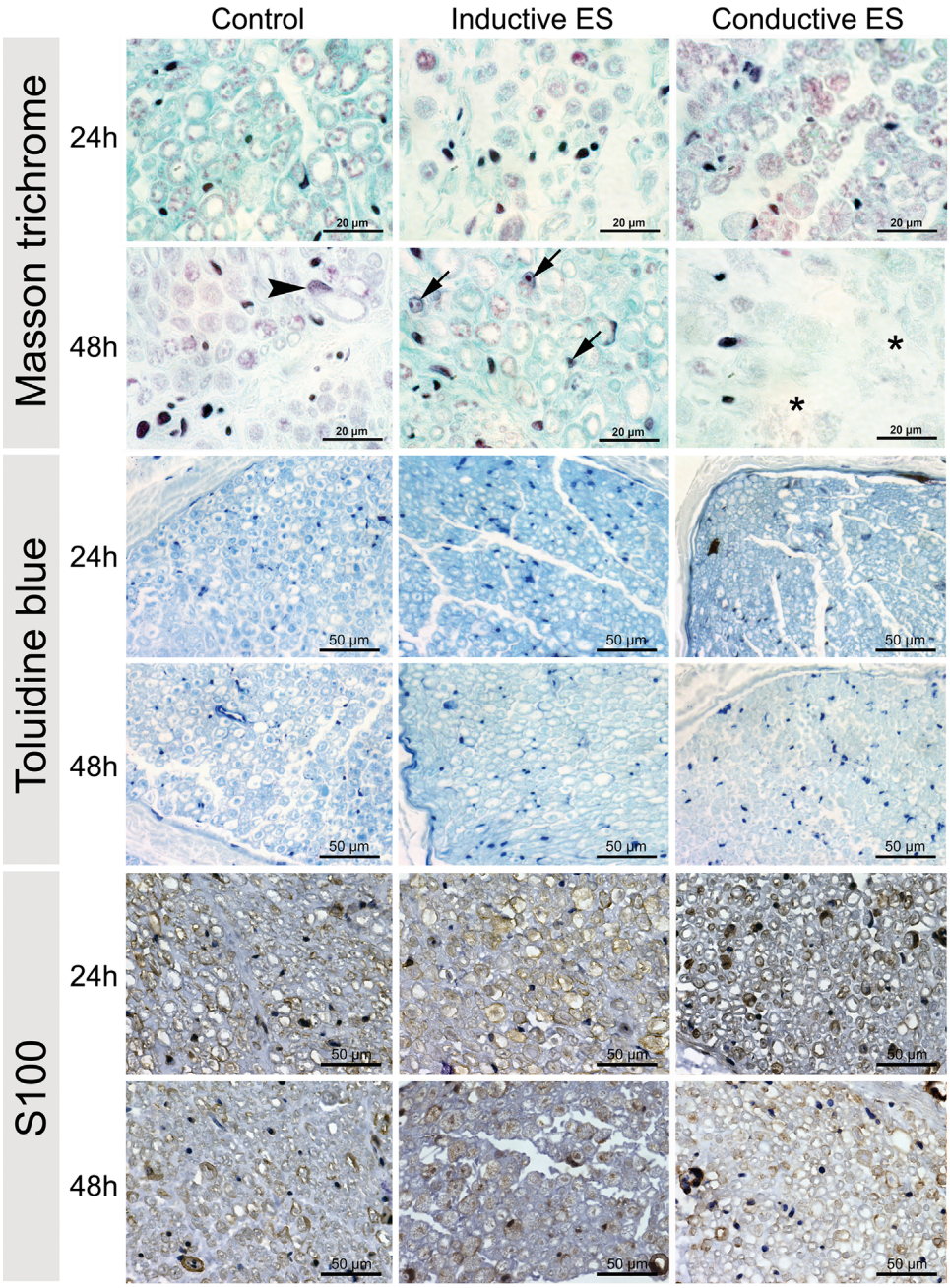

Fig. 2. Masson's trichrome staining ×1000: nuclear features in some investigated samples. Arrows indicate nuclei with well-shaped nucleoli of Schwann cells. Arrow head indicates swollen nuclei with condensed chromatine. Toluidine blue staining (×400): Weaker toluidine staining in the ES groups shows the rapid decrease of myelin or the accelerated Wallerian degeneration; S100 protein expression (×400): Intensive immunostaining of Schwann cells and occasional S100 deposits in axonal spaces. The strongest staining in the inductive ES groups reflects the highest cellularity occurrence.

Besides, an asymmetry of both Schwann cell and fibroblast distribution was found at the cross section of the stimulated nerve samples. Such an asymmetry appears as a higher cellularity on one half of the cross-section (side 1) than on the opposite half (side 2). The number of cells on both halves was evaluated by the same method described above and presented in Figure 3C. In contrast to the control group, the samples after ES revealed significant difference between two sides, of which the inductive ES recorded about twofold higher amount of cells on side 1 than on side 2, while the samples after conductive ES demonstrated lower cellularity but still significant asymmetric distribution. Noteworthy, similar patterns of bilateral asymmetry was detected in the immunolabelling of the proteins that predominantly demonstrated strong and moderate intracellular expression (N-CAM, FGF1, CNTF, NGF). However, despite their intracellular localisation, FGF2 as well as GDNF did not demonstrate visible asymmetry due to their strong expression in extracellular matrix, which was not

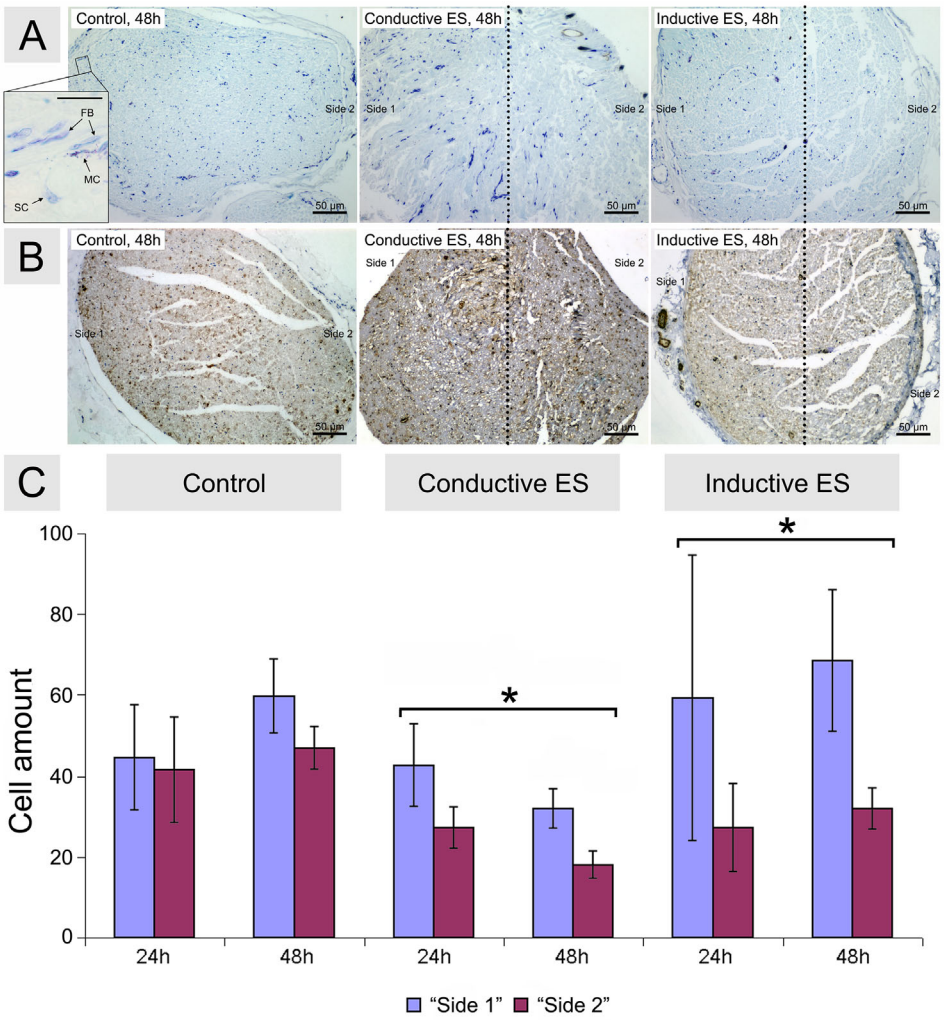

Fig. 3. Asymmetric bilateral cell distribution probably due to electrotaxis. (A) Cross-sections of sciatic nerves demonstrated higher cellularity on half (side 1) of the ES samples. ×100, toluidine blue staining. Insert shows the major cell populations: FB, fibroblasts; MC, mast cell; SC, neurolemmocyte (×1000, toluidine blue staining, scaling bar of 20 µm). (B) S100 immunolabeling revealed the bilateral asymmetry of Schwann cells in ES nerves. ×100. (C) Histogram revealed that the difference in cellularity between side 1 and side 2 is significant for all ES groups (*: conductive ES of 24 h, $P = 0.001$, DF = 8; conductive ES of 48 h, $P = 0.03$, DF = 2 (single sample, 6 fields of observations); inductive ES of 24 h, $P = 0.005$, DF = 8; inductive ES 48 h, $P = 2.1 \times 10^{-7}$, DF = 11; Error bar: standard deviation).

affected by ES and thus impeded visual evaluation of this phenomenon.

Cell proliferation. The proliferative potential of cells was determined as the percentage of Ki67-positive nuclei among the total nuclei of the same cell population. In general, all of the cell types demonstrated quite a low proliferative potential or were completely quiescent. That said, only the inductive ES group recorded a small yet definitely labeled amount of Ki67-positive Schwann cells and fibroblasts, particularly at 48 h (not shown). Worthy of mention is that in all of the Ki67-positive cells, Schwann cells and fibroblasts were found only in the periphery of the nerves, namely, within or immediately under the perineurium. However, this minuscule quantity of proliferating cells, which were predominantly found in nerves with inductive ES, did not enable us to calculate any meaningful proliferation index.

N-CAM (CD56). N-CAM expression has been shown to upregulate in the nerve stump distal to the injury following the switch of neurolemmocytes from myelinating to nonmyelinating phenotype (Fu and Gordon, 1997). The primary function of this cell-adhesion molecule is to guide the outgrowth of regenerating neurites. As shown in Figure 4, the intracellular expression of this marker was not only observed in Schwann cells but also in endothelial cells and fibroblasts. Similar to other markers, the presence of N-CAM was also detected in neurites. In addition, the immunostaining of connective tissue (perineurium) was constant at moderate intensity in each specimen under study. Among all of the groups, the intracellular expression in Schwann cells increased over time, with the inductive ES group exhibiting the strongest expression at 24 h and the conductive ES group displaying the lowest at 48 h. The axonal staining was less intense and more constant, with the inductive ES group again recording the strongest stain. Finally, the expression of this marker was found to closely correlate with the rate of Wallerian degeneration. Thus, inductive ES was found stimulate the expression N-CAM during Wallerian degeneration.

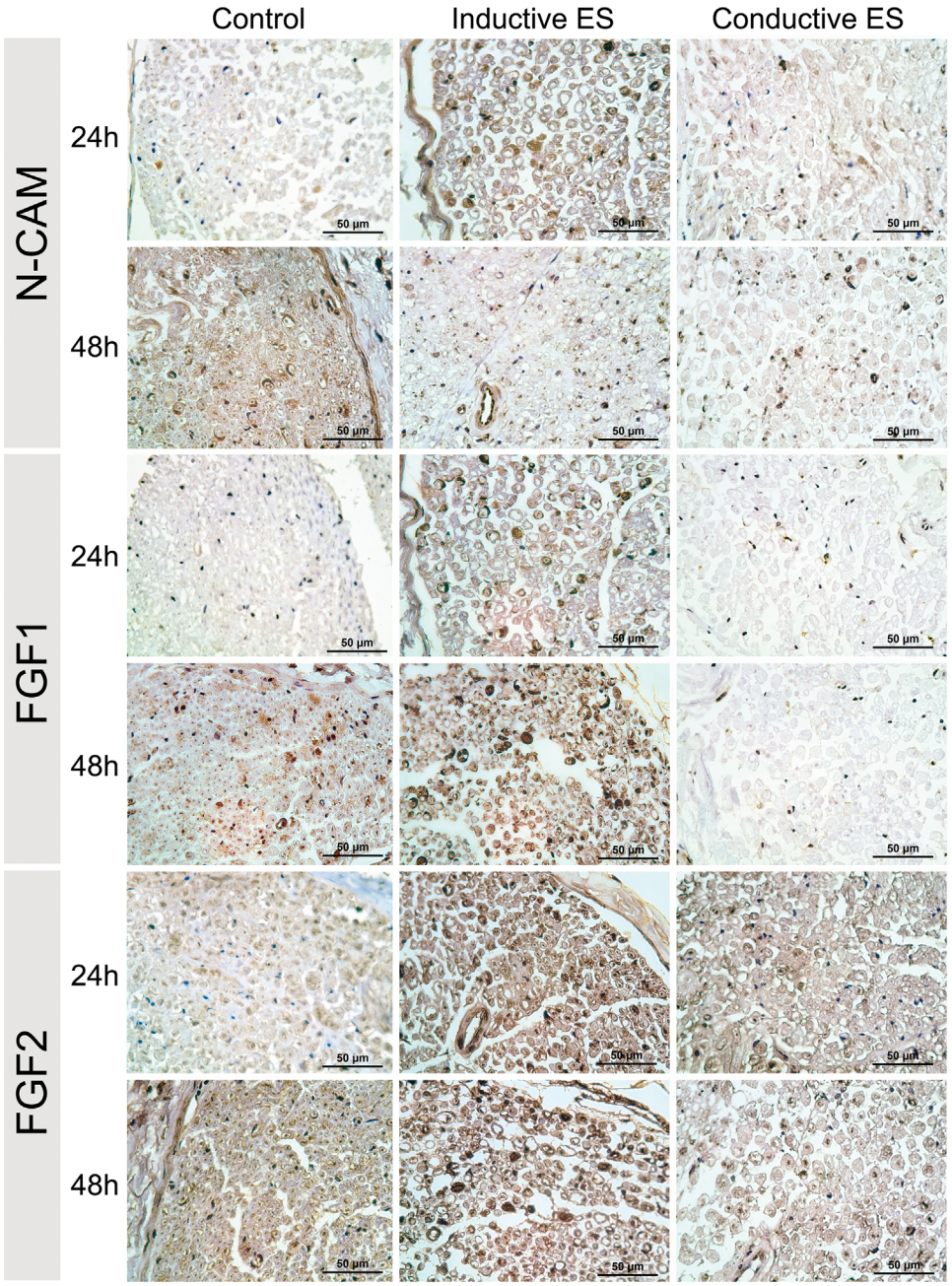

Fig. 4. Immunohistological stains of rat sciatic nerves after 24 and 48 h of tissue culture with or without ES. N-CAM: The cell adhesion proteins showed the progressively increased expression in the Schwann cells, particularly in the inductive ES groups at 24 h; FGF1: The samples following inductive ES displayed an increased expression of this marker; FGF2: Intense immunoexpression in all of the samples of the inductive ES groups.

Fibroblast Growth Factor 1 (FGF1). As a potent mitogen, FGF1 is expressed by macrophages, fibroblasts, endothelial cells and Schwann cells upon injury to promote angiogenesis and tissue regeneration (Raju et al., 2014). As shown in Figure 5, FGF1 was expressed by fibroblasts, endothelial cells, and Schwann cells both intra- and extracellularly. Among all of the groups, the highest and increasing expression was detected in the inductive ES samples, both intracellularly and in neurites. The control group demonstrated a weak expression at 24 h, becoming moderate to strong at 48 h. In contrast, the conductive ES group exhibited weak immunolabeling at both time points.

Fibroblast Growth Factor 2 (FGF2). Also a potent mitogen and an important growth factor promoting angiogenesis (Sonmez and Castelnuovo, 2014), FGF2 was strongly detected in every sample and in each important cell population, namely, fibroblasts, Schwann cells, and endothelial cells, as well as within the entire intercellular matrix in both the endo- and perineurium. There was, however, no significant difference in expression among the groups (Fig. 4).

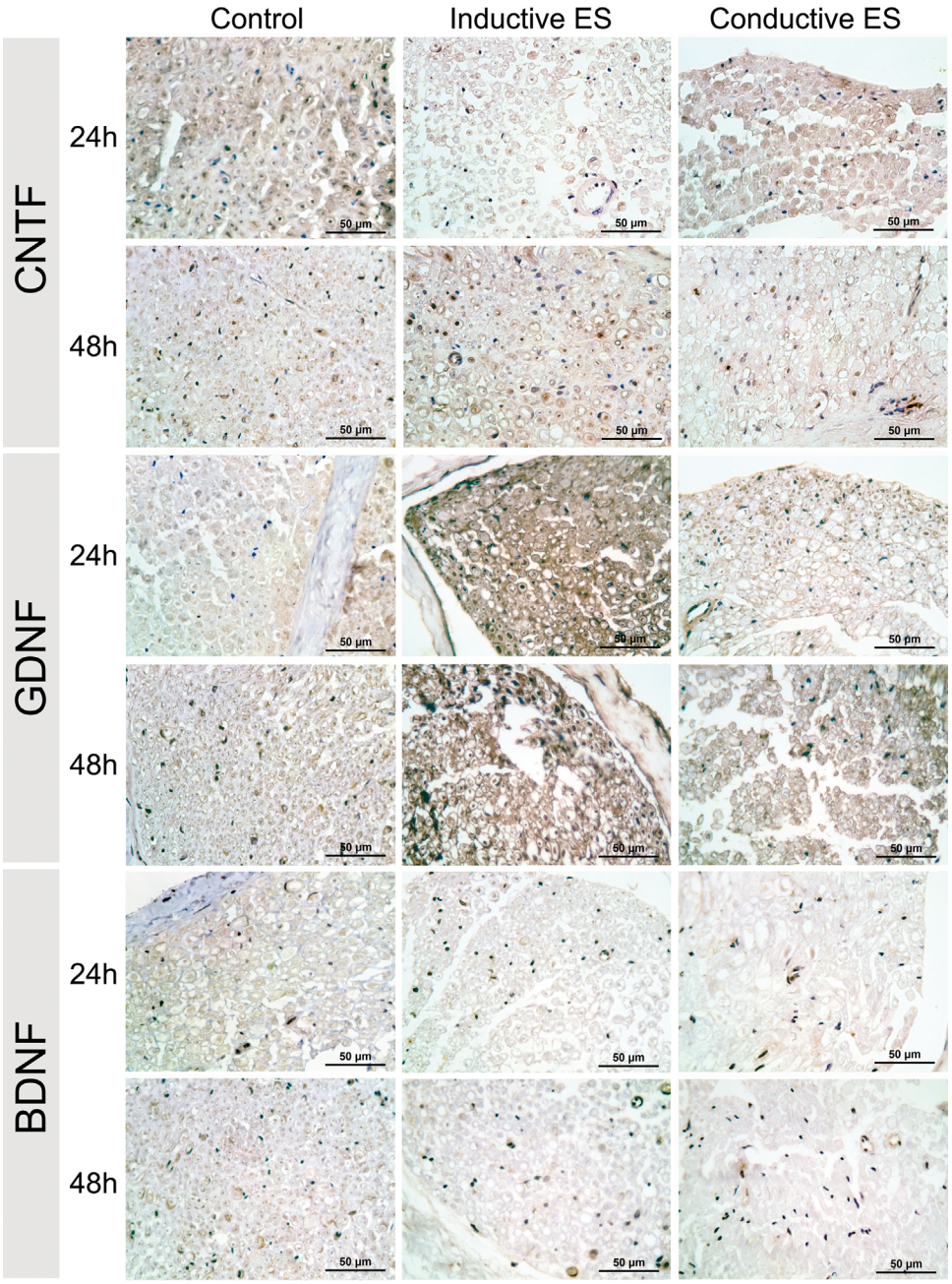

Fig. 5. Immunohistological stains of rat sciatic nerves after 24 and 48 h of tissue culture with or without ES. CNTF: Inductive ES induced a progressive increase in expression from moderate to strong in both the Schwann cells and the axons; GDNF: Strong expression in the inductive ES group after 24 and 48 h in both the Schwann cells and the axons; BDNF: Constant moderate expression in the controls and absence of axonal staining in each ES group.

Ciliary Neurotrophic Factor (CNTF). CNTF is a neuronal survival cytokine known to promote peripheral axon regeneration (Fu and Gordon, 1997). As shown in Figure 5, its most elevated expression in Schwann cells was found in the inductive ES samples in both periods of incubation, while both the conductive ES and the control groups exhibited a low level of intracellular CNTF expression. Although the axonal pattern of the CNTF immunostaining varied, the inductive ES group recorded the strongest expression at 48 h. Therefore the inductive ES was found more likely to stimulate CNTF secretion.

Glial Cell-Derived Neurotrophic Factor (GDNF). This factor is considered potent to neuronal survival and beneficial to axon regeneration (Fu and Gordon, 1997). Similar to other neurotrophins, GDNF was found in both Schwann cells and neurites, as shown in Figure 5. The inductive ES group demonstrated strong axonal and moderate to strong Schwann cell expression as early as 24 h and remained unchanged at 48 h.

The conductive ES group also showed constant moderate axonal expression at both time points. In contrast, the control group displayed no expression at 24 h, which increased from weak to moderate at 48 h.

Brain-Derived Growth Factor (BDNF). This neurotrophin has a complex function and is related to the regulation of neuron survival (Fu and Gordon, 1997). It was also found to increase the number of neurites in regenerating axons. In this study, the level of BDNF expression was not higher than moderate and had only a focal distribution in all of the groups, as shown in Figure 5. Interestingly, each ES group showed the absence of BDNF in axons. Schwann cell expression was found to be moderate or weak for the inductive ES and conductive ES groups, respectively.

Nerve Growth Factor (NGF). NGF belongs to the same family of neurotrophins as does BDNF and is critically important for the survival of sympathetic and sensory neurons. NGF also supports axonal outgrowth, branching, and elongation (Fu and Gordon, 1997). Negligible or weak focal NGF expression was generally found in most of the samples in both the neurites and Schwann cells. In contrast, the inductive ES group displayed a strong NGF expression in Schwann cells at 48 h and the axonal staining also appeared stronger in this group than in the other groups. Figure 6 presents the results.

NGF Receptor (p75). p75 or low affinity nerve growth factor receptor is upregulated in Schwann cells and motor neurons following denervation, probably related to accumulating and retrograding neurotrophins in the soma (Windebank and McDonald, 2005). This receptor is also associated with apoptosis. In contrast to other investigated markers, the expression of p75 was found only in the axial cylinders (Fig. 6). Furthermore, the staining intensity remained constantly weak despite increasing over time among all of the samples. Nevertheless, all of the stimulated samples showed lower level of p75 expression than the control group did.

Secretion of different growth factors by nerve cells

As shown in Figure 7, three out of four factors supported the tendency that the ES groups upregulated growth factor secretion. Of interest is the significant increase of CNTF secretion after 24 and 48 h of exposure to ES. GDNF secretion also increased but only after 48 h of exposure. FGF1 level in ES groups appeared higher than that in controls at both 24 h and 48 h, of which the difference was not statistically significant, however. Finally, NGF secretion remained unchanged.

Discussion

By this experimental model we attempted to demonstrate and explain the early stage of peripheral nerve repair after injury and, in particular, the influence of a well controlled ES on this process. Obviously, this ex vivo model excluded any anterograde transport from proximal nerve stump, and also

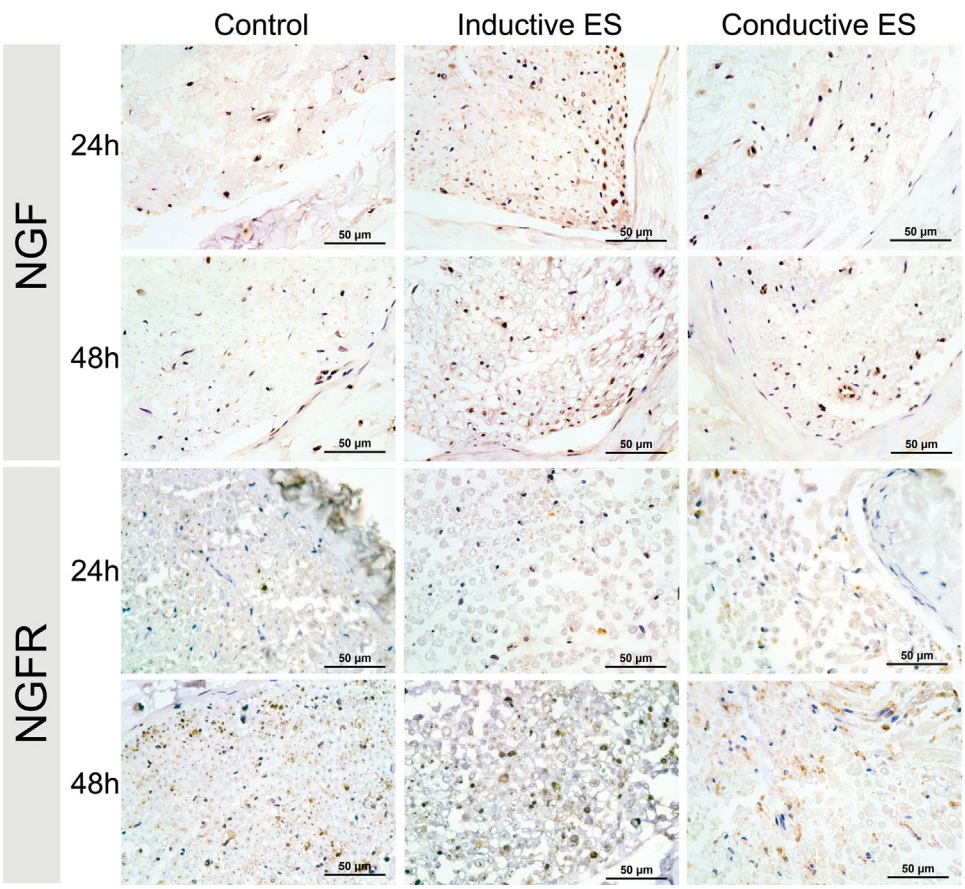

Fig. 6. Immunohistological stains of rat sciatic nerves after 24 and 48 h of tissue culture with or without ES. NGF: Negligible or weak expression in most samples, except for the strong presence in the Schwann cells following inductive ES; NGFR (p75): Weak yet increasing expression found only in the axons, particularly in the ES groups.

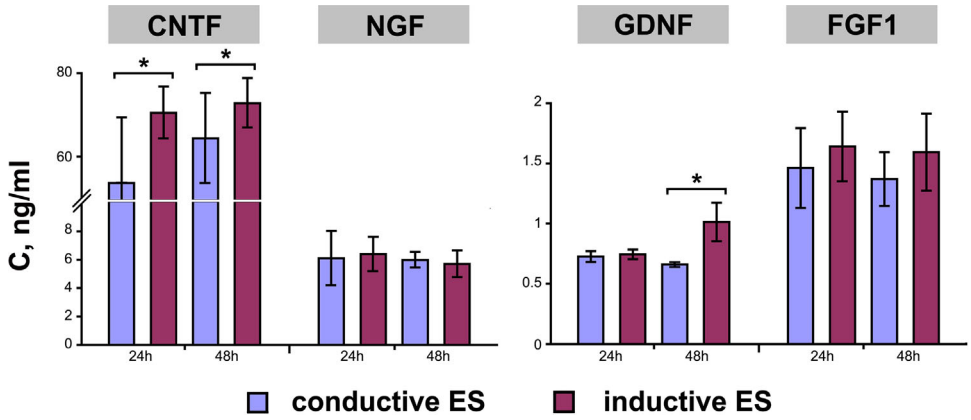

Fig. 7. ELISA data showing the general trend of increased expression following inductive ES and the significantly upregulated expression of CNTF and GDNF. C24 and C48: controls at 24 and 48 h. E24 and E48: inductive ES at 24 and 48 h. *: CNTF, C24 vs. E24, $P = 0.02$, DF = 10; C48 vs. E48, $P = 0.03$, DF = 14; GDNF, C48 vs. E48, $P = 3 \times 10^{-5}$, DF = 13.

cut off blood supply providing leukocytes that also help repairing the injured nerve. With these restrictions, this experimental model does permit to investigate the entire cell populations in peripheral nerve, Schwann cells and fibroblasts in particular, in their natural cellular environment and tissue scaffold under the influence of a well controlled electrical field (EF). Apparently, these conditions allow us to carefully evaluate how ES participates in the nerve regeneration process in a relatively realistic (vs. cell culture) and simplified (vs. animal experiment) environment. The data and parameters obtained in this model are hopefully useful to pre-clinic experiment design. Among the two models of ES, it was the inductive model that induced more conspicuous changes in most indicators measured at 24 h. Therefore the 48 h experiments were performed on the inductive nerve channels with the exception that a single nerve specimen was treated for 48 h by conductive ES.

Immediately following axotomy, important morphological changes and cellular activities take place in the nerve stump distal to the lesion to prepare for the regenerating axons from the proximal remaining nerve stump and to promote neuronal survival through retrograde transport (Allodi et al., 2012). In this work, distinct differences were found in the ES groups, particularly the inductive ES groups, with respect to the non-stimulated controls. These changes spanned a wide range of cellular features and activities, as is discussed below.

Cell activation and accelerated Wallerian degeneration

The higher number of Schwann cells in the ES groups and the proliferating neurolemmocytes and fibroblasts after 24 h of inductive ES indicate that ES, specifically inductive ES, accelerated the phenotype switch of Schwann cells from quiescent to proliferative. This Schwann cell activation and phenotype switching also accelerated Wallerian degeneration, as evidenced by the weaker myelin staining in all of the ES groups. Of interest is that this cell activation also included other major cell types, namely, fibroblasts and endothelial cells. Electrically activated fibroblasts are known to produce FGF1, FGF2 (Rouabhia et al., 2013), IL-2, and IL-6 (Shi et al., 2008) which are pro-angiogenic and pro-tissue repair. While S100 has been widely used as a general marker for Schwann cells, studies have reported weak and strong S100 stain and have suggested this activity to be associated with Schwann cell subpopulations (Garavito et al., 2000; Wewetzer, 2001). Another study associated S100 preferentially to the myelin-forming phenotype (Mata et al., 1990). In the present study, in light of the high number of S100-positive Schwann cells in the ES groups, the increased number of S100-positive Schwann cells in the control group between 24 and 48 h, and the relatively low number of Ki67-positive cells, it is suggested that this increase in S100-positive Schwann cell numbers is likely related to the phenotype switch rather than to cell proliferation. However, because the elevated number of S100-positive neurolemmocytes was not accompanied by strong myelin staining but rather the opposite, it is suggested that this process was related to the switching from stationary to migratory phenotype.

Another phenomenon of S100 immunoexpression in our study that demands explanation is its sporadic appearance within the axial cylinders, predominately after 48h of incubation. Considering neurite's normal localization within the axial cylinder formed by myelin sheaths, this finding gives the impression of S100-positive axoplasm, which is usually S100 negative (Mata et al., 1990). However, the specific conditions of our organ culture model (namely: axonal injury, culture in absence of blood and lymphatic circulation, ES) might shed light on this misconception. Axon degeneration in peripheral nerves usually occurs during the first 24 h after injury (Allodi et al., 2012). The interruption of axonal transport leads to the lack of the signaling molecules essential for axon survival, triggering axon disintegration (Conforti et al., 2014). The combination of factors, such as the increased permeability and destruction of axolemma, absence of fluid turnover together with enhanced Schwann cells' activity, may have resulted in the accumulation of different secreting molecules, particularly S100 protein, in neurite space. Eventually, this phenomenon could be considered as an additional evidence of accelerated Wallerian degeneration under ES.

Upregulated secretion of neurotrophins

ELISA data of the four factors from the inductive ES group confirm the general tendency, namely, higher expression in the ES groups, except for GDNF at 24 h and NGF at both time points. However, a significant upregulation was recorded only for CNTF at both time points and for GDNR at 48 h. In contrast to these four factors, the immunostaining revealed weak BDNF and FGF2 expression in all groups. To better understand such effect of ES on different trophic protein

expression it is important to remember the difference between ex vivo and in vivo models. In animal model, neurotrophins are not only generated by local cell populations but also supplied to the injury site through anterograde transport as well as produced by the leukocytes. Previous studies performed in animal models demonstrated high BDNF and FGF2 expression in response to ES (English et al., 2007; Geremia et al., 2007). Thus, this experimental model may allow us to distinguish those neurothrophins regulated autonomously in local injury from those that are predominantly delivered through axonal transport and/or by inflammatory cells. According to our results, we can conclude that the expression of at least three investigated growth factors (CNTF, GDNF, and FGF1) were upregulated by local cell populations in response to ES. Overall, inductive ES was found to be an effective approach to upregulate the expression of multiple neurotrophins, which is in line with the cellular activity following ES. ES has been shown to benefit axonal growth and reinnervation both in animal model (Mondello et al., 2014) and clinical experiments (Gordon et al., 2007).

Regulation of other molecules

Among all ten molecules, p75 is the only one to show a constant weaker expression following ES. p75 has been reported to mediate NGF-induced Schwann cell apoptosis (Petratos et al., 2003). In addition, this receptor was found to be upregulated during the dedifferentiation of Schwann cells upon axonal injury, ultimately reaching a peak in one month (Hirata et al., 2001), a phenomenon not observed in this study. One explanation is that the weak expression of p75 in this work is probably related to the experimental model which involved nerve tissue rather than a monolayer cell culture. Delayed p75 expression was also found in vivo compared to in vitro and was thought to be associated with other factors in tissue that suppressed p75 expression (Hirata et al., 2001). It is known that proliferative Schwann cells produce N-CAM to guide neurite growth; however, in this work a remarkably increased N-CAM expression was only observed at 24 h in the inductive ES group. Considering the expression of neurotrophic factors and p75, it is likely that ES differentially affected the expression of factors by Schwann cells, a potential modulating method to be further explored.

Morphological changes

The most obvious change is the increase in sample weight following ES; however, it is difficult to explain such phenomenon with total confidence. Theoretically, there are several ways to explain such weight increase. One probable cause is the interstitial oedema and cellular swelling associated with tissue injury. The routine histology revealed the presence of both, which however were not significantly different between the ES and control groups. Another cause may be due to cell proliferation. However, despite that morphometric analysis revealed almost two-fold more Schwann cells in all 24h-stimulated samples than in control group, further incubation almost equalized the difference. Moreover, Ki-67 expression in Schwann cells failed to show significant proliferative activity of any group. Nevertheless, the appearance of small but evident amount of Ki-67 positive Schwann cells and fibroblasts in the stimulated groups indicates that the ES protocols favours their proliferation and benefits the neuroregenerative process. The most probable hypothesis is the higher protein synthesis activity in the stimulated cells, which was supported by the remarkable nucleoli observed in Schwann cells and fibroblasts. Furthermore, enhanced protein production was proved immunohistochemically and by ELISA assay.

Another important morphological feature is the asymmetric cell distributions, i.e., the apparent migration of Schwann cells towards the perineurium and the high cellularity in one side of the nerve tissue. Theoretically, there were two important factors influencing cell migration: oxygen/nutrient gradient and electrotaxis. The volume of murine sciatic nerve (about 1 mm diameter) may cause diffusion gradient and so more oxygen and nutrients in the peripheral region than in the centre of the nerve stump, which may have provoked the migration of cells towards perineurium. In addition, the movement of cells in EF (electrotaxis) would have polarized cells towards one fabric "electrode" (inductive channels) and caused the cells to take side. For the conductive nerve channels there was no such polarized EF. However, the nerve stump may have adhered more tightly to one side of the channel because the channels were not perfectly circular. This may resulted in stronger ES to that side of the nerve tissue. EF may also change nutrient distribution inside the nerve tissue. Electrotaxis of different cell types has been reported in many studies (Funk et al., 2009; Levin, 2009). While it was not our objective to investigate the direction and speed of cell migration during ES, it is known however that electrotactic speed is quite variable and depends on current strength, cell type and environmental conditions, ranging from 4 to 6 μm/h for epidermal cells in vitro (Li et al., 2012) up to 100 μm/h for T-lymphocytes in vivo (Lin et al., 2008). These data virtually corresponded well with our experimental model in terms of the distance cells travelled. A potential benefit of high Schwann cell mobility is the promotion of phagocytosis and hence the clearance of myelin debris that permits Büngner band formation and axonal outgrowth. However, the asymmetric cell distribution remains an issue and should be avoided.

A potential pitfall in this nerve culture model is hypoxia in the center of the nerve tissue, which is a major concern in tissue and organ cultures (Freshney, 2000). Hypoxia usually leads to a downregulation of Schwann cell expression and induces their apoptosis, which was either not observed or very limited in this study. Moreover, a quantitative molecular analysis is complicated due to the variations in sample size and cell populations of different animals (Freshney, 2000). However, the highly limited cell apoptosis, the relatively higher cellularity in all of the ES samples, and the appearance of a small yet evident amount of Ki67-positive Schwann cells and fibroblasts in the inductive ES group all ultimately indicate that the tissue culture model in this work is suitable to study the neuroregenerative process. Longer culture times as well as investigation of genome activity in the ES responsive cell populations will evidently be warranted to further strengthen this conclusion.

The superior efficacy of the inductive channels obtained under the current ES parameters does not exclude the potential of the conductive channels. The ES intensities used in the two models are slightly different, i.e., 160 mV/mm for the conductive model and 200 mV/mm for the inductive model. However, since the EF gradient and distribution inside the two models are very different, the efficacy of these two models can not be compared simply based on the nominal ES intensity. We believe that under the current ES parameters the configuration of the nerve channels is the deciding factor of the observed difference between the two types of channels. Nevertheless, this highlights the importance of theoretical calculation of EF inside tissues and culture medium according to different ES configurations.

Conclusions

This study presented a novel ex vivo tissue culture model to study denervated axon in electrical field. The PPy-coated PET fabric channels are capable of distributing pulsed ES to

effectively accelerate the first phase of neuroregeneration, namely, Wallerian degeneration, Schwann cell phenotype switch and upregulated secretion of CNTF, GDNF and FGF1. Furthermore, this work demonstrated the autonomous regulation of peripheral nerve healing by growth factors independent of the central nerve system. In addition, it is demonstrated for the first time that EF can induce cell migration inside axon, highlight the importance of adequate design of EF distribution in axon when ES is used. As this ES process took place in the original nerve tissue architecture in the presence of other cell populations, the experimental parameters and data provide relevant reference to in vivo study.

Acknowledgments

This work was supported by The Canadian Institutes of Health Research Operating Grant (MOP 106555) and the Centre de recherche du CHU de Québec. DW wants to thank the salary support of the China Scholarship Council.

Literature Cited

Allodi I, Udina E, Navarro X. 2012. Specificity of peripheral nerve regeneration: Interactions at the axon level. Prog Neurobiol 98:16–37.

Balint R, Cassidy NJ, Cartmell SH. 2014. Conductive polymers: Towards a smart biomaterial for tissue engineering. Acta Biomater 10:2341–2353.

Conforti L, Gilley J, Coleman MP. 2014. Wallerian degeneration: An emerging axon death pathway linking injury and disease. Nat Rev Neurosc 15:394–409.

English AW, Schwartz G, Meador W, Sabatier MJ, Mulligan A. 2007. Electrical stimulation promotes peripheral axon regeneration by enhanced neuronal neurotrophin signaling. Dev Neurobiol. 67:158–172.

Fawcett JW, Keynes RJ. 1990. Peripheral nerve regeneration. Annu Rev Neurosci 13:43–60.

Forciniti L, Ybarra J, 3rd, Zaman MH, Schmidt CE. 2014. Schwann cell response on polypyrrole substrates upon electrical stimulation. Acta Biomater 10:2423–2433.

Freshney RI. 2000. Culture of animal cells: A manual of basic techniques—4th ed. New York: Wiley-Liss, pp 395–399.

Fu SY, Gordon T. 1997. The cellular and molecular basis of peripheral nerve regeneration. Mol Neurobiol 14:67–116.

Funk R, Monsees T, Özkucur N. 2009. Electromagnetic effects—From cell biology to medicine. Prog Histochem Cytochem 43:177–264.

Garavito ZV, Sutachán JJ, Muñetón VC, Hurtado H. 2000. Is S-100 protein a suitable marker for adult Schwann cells? In Vitro Cell Dev Biol Anim 36:281–283.

Geremia NM, Gordon T, Brushart TM, Al-Majed AA, Verge VM. 2007. Electrical stimulation promotes sensory neuron regeneration and growth-associated gene expression. Exp Neurol 205:347–359.

Gordon T, Brushart TM, Amirjani N, Chan KM. 2007. The potential of electrical stimulation to promote functional recovery after peripheral nerve injury-comparisons between rats and humans. Acta Neurochir Suppl 100:3–11.

Gordon T, Chan KM, Sulaiman OA, Udina E, Amirjani N, Brushart TM. 2009. Accelerating axon growth to overcome limitations in functional recovery after peripheral nerve injury. Neurosurgery 65:A132–A144.

Hirata H, Hibasami H, Yoshida T, Ogawa M, Matsumoto M, Morita A, Uchida A. 2001. Nerve growth factor signaling of p75 induces differentiation and ceramide-mediated apoptosis in Schwann cells cultured from degenerating nerves. Glia 36:245–258.

Huang J, Lei Lu, Jianbin Zhang, Xueyu Hu, Yongguang Zhang, Wei Liang, Siyu Wu, Zhuojing Luo.. 2012. Electrical stimulation to conductive scaffold promotes axonal regeneration and remyelination in a rat model of large nerve defect. PloS ONE 7:e39526.

Jiang HH, Gill BC, Dissaranan C, Zutshi M, Balog BM, Lin D, Damaser MS. 2013. Effects of acute selective pudendal nerve electrical stimulation after simulated childbirth injury. Am J Physiol Renal Physiol 304:F239–F247.

Koppes AN, Seggio AM, Thompson DM. 2011. Neurite outgrowth is significantly increased by the simultaneous presentation of Schwann cells and moderate exogenous electric fields. J Neural Eng 8:046023.

Levin M. 2009. Bioelectric mechanisms in regeneration: Unique aspects and future perspectives. Sem Cell Dev Biol 20:543–556.

Li L, Gu W, Du J, Reid B, Deng X, Liu Z, Zong Z, Wang H, Yao B, Yang C, Yan J, Zeng L, Chalmers L, Zhao M, Jiang J. 2012. Electric fields guide migration of epidermal stem cells and promote skin wound healing. Wound Rep Reg 20:840–851.

Lin F, Baldessari F, Gyenge CC, Sato T, Chambers RD, Santiago JG, Butcher EC. 2008. Lymphocyte Electrotaxis in vitro and in vivo. J Immunol 181:2465–2471.

Luo B, Huang J, Lu L, Hu X, Luo Z, Li M. 2014. Electrically induced brain-derived neurotrophic factor release from Schwann cells. J Neurosci Res 92:893–903.

Marquardt LM, Sakiyama-Elbert SE. 2013. Peripheral nerve repair. Curr Opin Biotechnol 24:887–892.

Mata M, Alessi D, Fink DJ. 1990. S100 is preferentially distributed in myelin-forming Schwann cells. J Neurocytol 19:432–442.

Mondello SE, Kasten MR, Horner PJ, Moritz CT. 2014. Therapeutic intraspinal stimulation to generate activity and promote long-term recovery. Front Neurosci 8:21.

Nguyen HT, Wei C, Chow JK, Nguy L, Nguyen HK, Schmidt CE. 2013. Electric field stimulation through a substrate influences Schwann cell and extracellular matrix structure. J Neural Eng 10:046011.

Petratos S, Butzkueven H, Shipham K, Cooper H, Bucci T, Reid K, Lopes E, Emery B, Cheema SS, Kilpatrick TJ. 2003. Schwann cell apoptosis in the postnatal axotomized sciatic nerve is mediated via NGF through the low-affinity neurotrophin receptor. J Neuropathol Exp Neurol 62:398–411.

Raju R, Palapetta SM, Sandhya VK, Sahu A, Alipoor A, Balakrishnan L, Advani J, George B, Kini KR, Geetha NP, Prakash HS, Prasad TS, Chang YJ, Chen L, Pandey A, Gowda H. 2014. A Network Map of FGF-1/FGFR Signaling System. J Signal Transduct 2014: 962962.

Rouabhia M, Park H, Meng S, Derbali H, Zhang Z. 2013. Electrical stimulation promotes wound healing by enhancing dermal fibroblast activity and promoting myofibroblast transdifferentiation. PLoS One 8:e71660.

Scherer SS, Salzer JL. 2001. Axon-Schwann cell interactions during peripheral nerve degeneration and regeneration. KR Jessen and WD Richardson, eds. 2nd Ed., Glial cell development. London: Oxford University Press, pp 299–330.

Shi G, Zhang Z, Rouabhia M. 2008. Reregulation of cell functions electrically using biodegradable polypyrrole-polylactide conductors. Biomaterials 29:3792–3798.

Sonmez AB, Castelnuovo J. 2014. Applications of basic fibroblastic growth factor (FGF-2, bFGF) in dentistry. Dent Traumatol 30:107–111.

Wallace GG, Spinks GM, Kane-Maguire LAP, Teasdale PR. 2003. Conductive electroactive polymers: intelligent materials systems. 2nd Ed., Boca Raton: CRC Press.

Wang Y, Rouabhia, Zhang Z. 2013. PPy-coated PET fabrics and electric pulse-stimulated fibroblasts. J Mater Chem B 1:3789–3796.

Wewetzer K. 2001. Response to Gavarito, Z. V; Muneton, V. C; Sutachán, J. J; Hurtado, H. Is S-100 protein a suitable marker for adult Schwann cells? (In Vitro Cell. Dev. Biol. 36a:281-283; 2000). In Vitro Cell Dev Biol Anim 37:89.

Windebank AJ, McDonald ES. 2005. Neurotrophic factors in the peripheral nervous system. In: Dyck PJ, Thomas PK, editors. Peripheral neuropathy, 4th edn. Philadelphia: Elsevier Saunders, Chapter 17, pp 377–386.

Zhang Z, Rouabhia M, Wang Z, Roberge C, Shi G, Roche P, Li J, Dao LH. 2007. Electrically conductive biodegradable polymer composite for nerve regeneration: Direct current stimulated neurite outgrowth and axon regeneration. Artif Organs 31:13–22.